

Original Research Article

Same-day consultation, simulation and lung Stereotactic Ablative Radiotherapy delivery on a Magnetic Resonance-linac

Miguel A. Palacios*, Sonja Verheijen, Famke L. Schneiders, Omar Bohoudi, Berend J. Slotman, Frank J. Lagerwaard, Suresh Senan

Amsterdam UMC, Vrije Universiteit Medical Centre, Dept. of Radiation Oncology, de Boelelaan 1117, 1081 HV Amsterdam, the Netherlands



ARTICLE INFO

Keywords:

Lung SBRT
Same-day treatment
Single Fraction
MR-guided
Intra-fraction
Motion Management
Breath-hold

ABSTRACT

Background and Purpose: Magnetic resonance-guided radiotherapy (MRgRT) with real-time intra-fraction tumor motion monitoring allows for high precision Stereotactic Ablative Radiotherapy (SABR). This study aimed to investigate the clinical feasibility, patient satisfaction and delivery accuracy of single-fraction MR-guided SABR in a single day (one-stop-shop, OSS).

Methods and Materials: Ten patients with small lung tumors eligible for single fraction treatments were included. The OSS procedure consisted of consultation, treatment simulation, treatment planning and delivery. Following SABR delivery, patients completed a reported experience measure (PREM) questionnaire. Prescribed doses ranged 28–34 Gy. Median GTV was 2.2 cm³ (range 1.3–22.9 cm³). A gating boundary of 3 mm, and PTV margin of 5 mm around the GTV, were used with auto-beam delivery control. Accuracy of SABR delivery was studied by analyzing delivered MR-cines reconstructed from machine log files.

Results: All 10 patients completed the OSS procedure in a single day, and all reported satisfaction with the process. Median time for the treatment planning step and the whole procedure were 2.8 h and 6.6 h, respectively. With optimization of the procedure, treatment could be completed in half a day. During beam-on, the 3 mm tracking boundary encompassed between 78.0 and 100 % of the GTV across all patients, with corresponding PTV values being 94.4–100 % (5th–95th percentiles). On average, system-latency for triggering a beam-off event comprised 5.3 % of the delivery time. Latency reduced GTV coverage by an average of –0.3 %. Duty-cycles during treatment delivery ranged from 26.1 to 64.7 %.

Conclusions: An OSS procedure with MR-guided SABR for lung cancer led to good patient satisfaction. Gated treatment delivery was highly accurate with little impact of system-latency.

1. Introduction

Stereotactic ablative radiation therapy (SABR) is now a standard of care for patients with early-stage small volume thoracic tumors [1,2], with many authors reporting long-term local control rates of approximately 90 %. The cornerstones for SABR are: 1) target localization; 2) treatment planning and dose calculation; and 3) tumor motion management during treatment delivery [3].

Furthermore, SABR delivered in a single fraction can improve patient convenience and decrease costs. To date, three clinical studies have shown that single fraction SABR for lung tumors is equivalent to fractionated SABR in terms of toxicity, local control (LC), progression free survival (PFS) and overall survival (OS) [4–6]. None of the three studies reported grades 4–5 toxicity events. In addition, no differences in clinical outcomes have been observed when delivering single fractions of

either 30 Gy or 34 Gy to lung lesions [7].

Novel techniques for lung SABR, such as MR-guided radiotherapy and protons, have attracted much interest [8–12]. MR-guided radiotherapy allows use of online plan adaptation according to the anatomy of the day, and real-time imaging of tumor position and gated delivery [8,9,12,13]. Following the introduction of MR-guided single fraction (SF) lung SABR [14], the present study was performed to investigate clinical feasibility, patient satisfaction and the delivery accuracy of a one-stop-shop (OSS) service for MR-guided lung SABR. Similar procedures are well known in the palliative setting [15,16], but to our knowledge it has never been implemented for single fraction MR-guided SABR delivery. We report on the main steps required for this procedure, the accuracy and efficiency of treatment delivery and on the patient reported experience measures (PREMs) after completion of the treatment.

* Corresponding author.

<https://doi.org/10.1016/j.phro.2022.09.010>

Received 9 August 2022; Received in revised form 26 September 2022; Accepted 27 September 2022

Available online 3 October 2022

2405-6316/© 2022 The Authors. Published by Elsevier B.V. on behalf of European Society of Radiotherapy & Oncology. This is an open access article under the CC BY-NC-ND license (<http://creativecommons.org/licenses/by-nc-nd/4.0/>).

Table 1

Patient characteristics. Range of motion was calculated using the maximum displacement of the centroid of the GTV as observed in the acquired MRI cines during simulation.

Patient	GTV (cc)	Tumor Location (lobe)	AP (cm)	CC (cm)	LR (cm)	Dose prescription	Breath-Hold
1	4.1	Left Inf.	0.6	2.8	0.5	1x34 Gy	Insp.
2	1.3	Left Inf.	0.3	2.5	0.1	1x34 Gy	Insp.
3	2.4	Right Sup.	0.5	0.8	0.3	1x30 Gy	Insp.
4	1.7	Right Sup.	1.3	1.5	0.3	1x34 Gy	Insp.
5	2.3	Right Sup.	0.9	1.6	0.1	1x30 Gy	Insp.
6	1.5	Left Inf.	0.7	2.2	0.2	1x30 Gy	Insp.
7	22.9	Right Med.	0.6	1.7	0.4	1x34 Gy	Insp.
8	3.2	Left Inf.	0.7	2.0	0.2	1x28 Gy	Insp.
9	2.0	Right Med.	0.7	1.6	0.2	1x34 Gy	Insp.
10	1.3	Right Inf.	0.5	2.2	0.2	1x30 Gy	Exp.

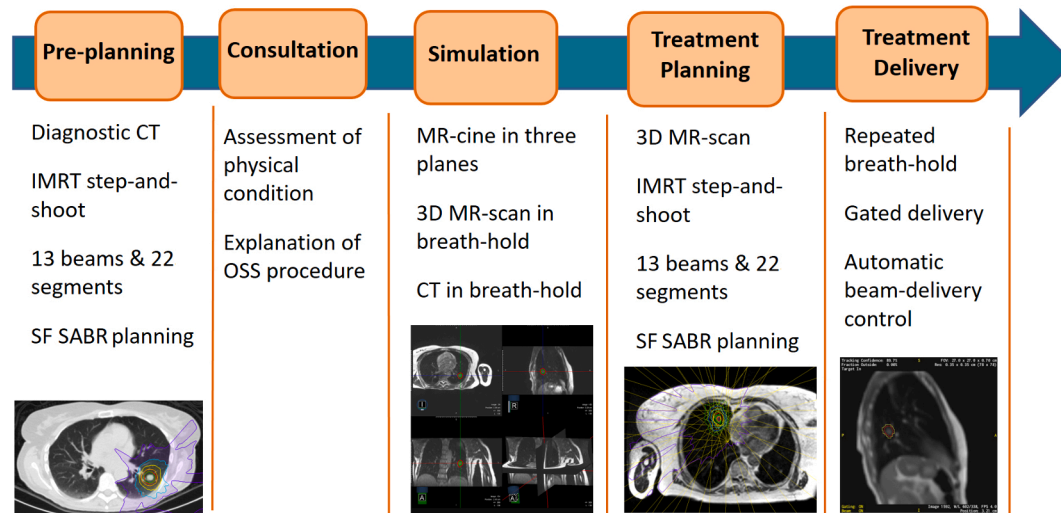


Fig. 1. Steps in the clinical workflow for the simulation, planning and treatment delivery of one-stop-shop single-fraction (SF) lung SABR.

2. Material and Methods

2.1. Patient characteristics

Ten prospective consecutive patients were identified as suitable for the OSS lung SF SABR procedure. Informed consent was obtained from all patients, and this study has been exempted by the VU University Medical Center Medical Ethics Review Committee (#2018.602, IRB00002991). Excluded were tumors > 5 cm in diameter, tumors involving central pleural and/or structures of the mediastinum and finally, tumors touching the zone of the proximal bronchial tree. No other selection criteria were followed than patient fitness and understanding of the procedure. Patient characteristics are summarized in [Table 1](#). The median GTV size was 2.2 cm³ (range, 1.3–22.9 cm³). Median patient age at the time of treatment was 71 years (range, 63–85 years). Dose prescription was 1x28Gy for one patient with metastatic disease, 1x30Gy for 4 patients (small tumors or adjacent to the chest wall) and 1x34Gy for 5 patients. Each patient was asked at the end of OSS procedure to fill in a PREM to evaluate the overall patient satisfaction for this treatment option.

2.2. MR-guided OSS lung workflow

2.2.1. Pre-planning

Prior to the OSS procedure, a telephone consultation took place between the radiation oncologist and patient to explain the procedure and ascertain the fitness of the patient to complete it in a single day. A general overview of the full procedure can be seen in [Fig. 1](#). For three patients, a pre-treatment planning on an available diagnostic CT-scan

was performed prior to the date of the OSS procedure in order to reduce the time required for treatment planning on the day of treatment.

2.2.2. Consultation and Simulation

On the day of the OSS procedure, an in-person consultation with the radiation oncologist took place. Next, the patient underwent an MR simulation with the MRIdian system (ViewRay Inc., Mountain View) operating at 0.35 T, consisting in the acquisition of at least one 3D MR scan in shallow inspiration/expiration breath-hold. The 3D MR scan was based on a true FISP sequence (Siemens) acquisition with FOV 45 cm × 45 cm × 24 cm, resolution 0.16 cm × 0.16 cm × 0.30 cm, TR/TE of 3.83/1.62 ms and Flip Angle (FA) of 60°. Subsequently, tumor motion characteristics were determined using a series of MR-cines in sagittal, coronal and axial planes. Repeated breath-hold instructions were given in order to ascertain the understanding and compliance of the patient with breath-hold procedures. MR-cines were acquired at a frequency of 3 frames per second (fps) with a 0.7 cm slice thickness, variable FOV depending of the orientation, in-plane resolution of 0.30 cm × 0.30 cm, average TR/TE of 2.5/1.1 ms and Flip Angle of 45° ([Supplementary Fig. 1](#), illustrates variations in lung tumor contrast according to the FA). The GTV was then delineated on the most representative sagittal plane of the 3D MR acquisition, followed by assessment of automatic tumor contour “tracking” (or automatic GTV delineation) by the MRIdian software on a new sagittal MR-cine in order to mimic treatment delivery. Usually, a sagittal plane through the mid-section of the tumor was chosen. During this last step, an in-room MR compatible monitor was used to display the real-time MR cine frames with the projection of the GTV and tracking boundary contours to assist the patient during breath-holds [13]. The decision gating in either inspiration or expiration

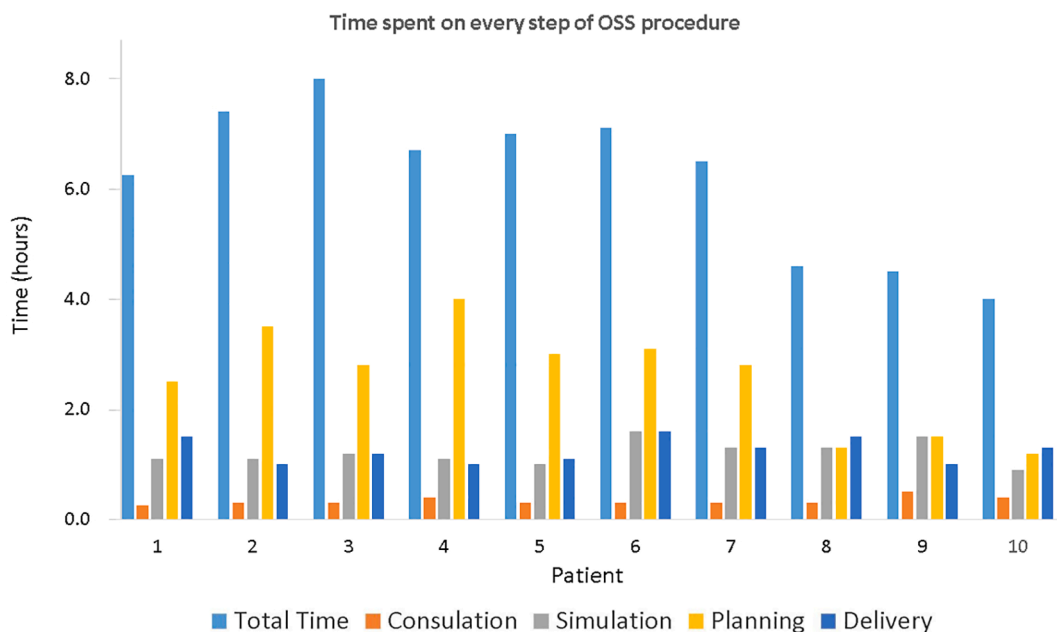


Fig. 2. Time spent on each step of the one-stop-shop (OSS) procedure for the 10 patients included in the study.

breath-hold was made on the basis of patient convenience and compliance, as well as a visual assessment of the automatic tumor contour “tracking”.

After the MRI simulation procedure, the 3D MR was imported into the MRIdian treatment planning system (ViewRay Inc., Mountain View), for delineation of target and OARs. Delineation of the OARs was performed semi-automatically with the use of deformable image registration (DIR), either by using an atlas-based database within the MRIdian or the delineations previously completed on the diagnostic CT. The database was formed using templates from representative patients treated at the MRIdian in the past or with the delineations previously performed on the diagnostic CT. During the OSS procedure, the Advanced Registration Module in the MRIdian TPS was used and Volume Of Interest (VOI) around the different OAR structures were placed to increase the accuracy of the registration. The MR-simulation was followed by a CT-scan in the selected breath-hold state and subsequently imported in the MRIdian TPS. The CT-scan was first rigidly registered with the MRIdian 3D MR primary image and the GTV was delineated on the fused image. The MRI-based delineated GTV contour was compared with the CT-based contour and adjusted at the discretion of the physician. The CT-scan underwent a second DIR-based registration to the planning 3D MR scan to generate an electron density map for accurate dose calculation.

2.2.3. Treatment planning

Treatment plans were generated with the MRIdian TPS consisting of an average of 13 IMRT step-and-shoot beams, and 22 segments. For all patients, a PTV margin of 5 mm around the GTV was generated to account for intra-fraction residual motion and possible microscopic tumor spread around the GTV. In addition, a structure of 3 mm was employed around the GTV to serve as a gating boundary. All treatment plans were normalized to cover 95 % of the PTV by the prescription dose (PD) and the near-maximum dose was allowed to be escalated to 140 % of the PD. Main organs at risk (OAR) constraints used were: Chest wall Dmax < 30 Gy & 1.0 cc @ 22 Gy; Spinal Cord Dmax < 14 Gy & 0.35 cc @ 10 Gy; Remaining soft tissue 0.1 cc @ 15 Gy.

After approval of the treatment plan, patients returned to the treatment vault and were positioned on the couch. A new 3D MR scan with the same protocol as for the simulation was acquired to ensure patient alignment, with care taken to reproduce the same breath-hold depth as

during the simulation. The newly acquired 3D MR scan was rigidly registered to that of the treatment planning, and when needed, GTV and OARs contours were adapted to correct for possible rotations. A new plan was generated based on the actual anatomy, by using the same beam configuration and objectives as in the original treatment plan. After an online patient-specific quality assurance (QA) step was performed with a secondary Monte Carlo (MC) dose calculation algorithm, the plan was reviewed and approved by the radiation oncologist. Next, the most representative sagittal plane was selected for use as original Key Frame with the GTV and Boundary contour information.

2.2.4. Treatment delivery

Treatment delivery proceeded with repeated breath-hold in two consecutive sessions with real-time visual feedback of actual GTV position. During each session, half of the PD was delivered with a pause in between to allow the patient to rest between both sessions. During delivery, continuous MR-cine in a sagittal plane at 4 fps was acquired with FOV 0.35 cm × 0.35 cm, 0.7 cm slice thickness, TR/TE: 2.1/0.9 ms, and FA of 60°.

2.3. Intra-fraction motion management

Before starting beam-on, the Key Frame was updated with a sagittal frame from the MR-cine after careful inspection of the projected GTV contour. Each new frame was subsequently deformable registered to this newly selected Key Frame. The system automatically processes each image and triggers a beam on/off depending on the amount of GTV outside of the Boundary (usually threshold of > 10 % in our OSS procedure) and a Confidence Value (CV) metric set as high as possible (threshold at least > 0.80). The Confidence Value is calculated as a weighted summation of the evaluation of the registration performed by each tracker composing the DIR algorithm during real-time delivery. A high Confidence Value means that the DIR algorithm sees that the two images are quite similar to each other and is confident about the tracking result and the gating decision. During treatment delivery the following states are possible:

- Gating ON/Beam ON: both thresholds for GTV ∩ Boundary overlap and CV are satisfied and beam is on.

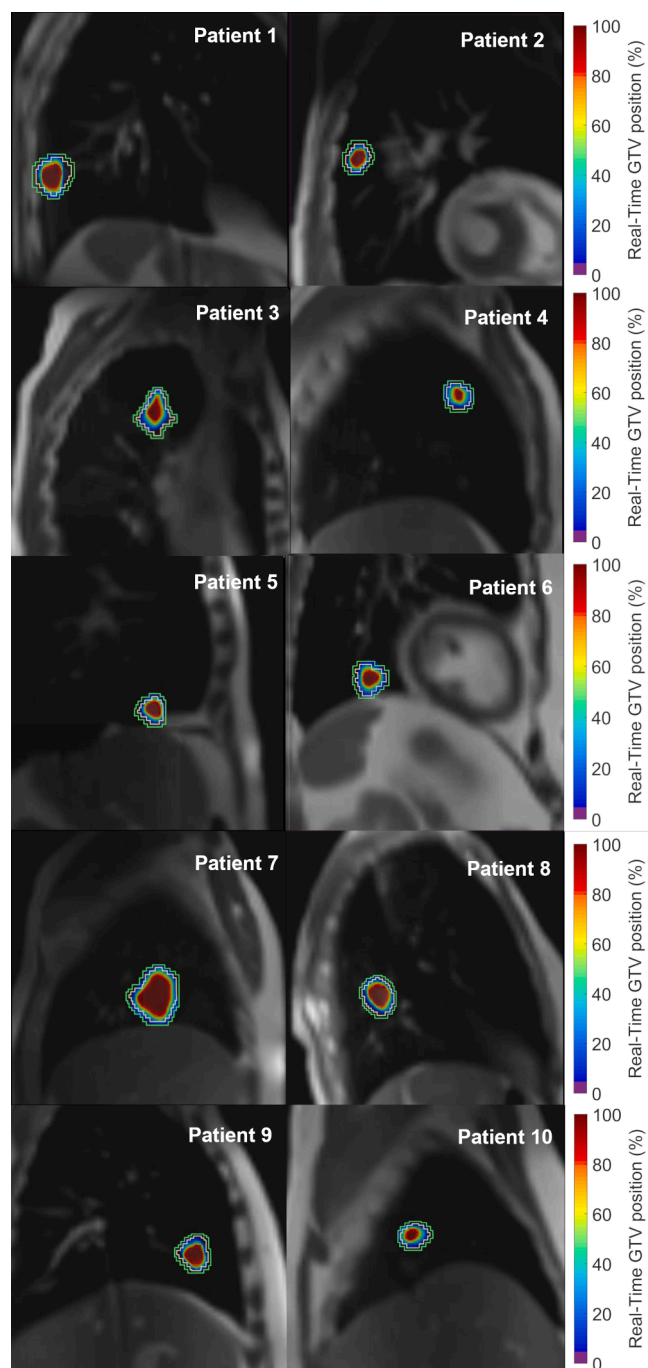


Fig. 3. Heatmaps of the real-time position of the GTV during gated treatment delivery for the 10 one-stop-shop lung SABR patients. Boundary and PTV contours are shown in light yellow and green, respectively.

- Gating OFF/Beam OFF: at least one of the two thresholds is not satisfied and a beam-off is triggered.
- Gating ON/Beam OFF: both thresholds are satisfied but the beam is still off because previous frames had led to a beam-off and system-latency (first frame resulting again in a gating ON decision).
- Gating OFF/Beam ON: at least one of the two thresholds is not satisfied, but due to gating and system latency, the beam is still on.

2.4. Post-treatment analyses of gating performance

Delivered MR-cines reconstructed from machine log files were analysed, which contained information about the gating decisions and beam

Table 2

Gating results extracted from the treatment delivery of the 10 OSS patients. The dose was delivered in two consecutive parts, during which patient tolerance was assessed.

Patient	ROI (%) Part1/ Part2	GTV \cap Boundary 5th–95th	GTV \cap PTV 5th–95th	Latency Effect Mean(%)	Duty-Cycle (%)	% Frames Latency ON-OFF/ OFF-ON
1	10/10	85.7–100	96.4–100	–0.5	43.3	7.8/4.7
2	10/10	87.9–100	100–100	–0.2	57.3	12.5/5.2
3	10/10	89.2–100	99.0–100	–0.2	64.7	18.1/8.2
4	15/15	80.0–100	97.8–100	–0.5	40.8	11.7/8.2
5	10/10	91.1–100	100–100	0.0	43.8	4.2/2.2
6	10/10	78.0–100	94.4–100	–0.8	35.6	7.6/5.6
7	10/10	89.1–100	96.2–100	–0.4	51.5	13.0/5.8
8	10/10	90.8–100	99.2–100	–0.2	41.3	5.3/2.8
9	10/7	93.1–100	99.8–100	–0.1	39.8	7.0/4.3
10	10/15	83.1–100	98.5–100	–0.5	26.1	8.6/5.9

ROI(%): threshold used to trigger automatic beam-off when the GTV is outside the Boundary. For the majority of patients a threshold of 10% was used. To increase the efficiency, for two patients a threshold of 15% was used.

GTV \cap Boundary/PTV: amount of overlap between the GTV and Boundary/PTV during beam-on.

Latency Effect: mean decrease in the overlap of GTV with Boundary/PTV as a result of beam latency (Gating Off/Beam On).

Duty-Cycle: efficiency during treatment delivery (ratio of beam-on time to total time).

% Frames latency: percentage of frames affected by beam latency (Gating On/Beam Off, and Gating Off/Beam On).

on/off status. A total of 81,445 frames (5.65 h) were collected for the 10 patients included. Information of the GTV contour and Boundary was available on each frame. Each frame was converted to.jpeg format and read as RGB image in MATLAB (version 2018b, The MathWorks Inc., Natick, Massachusetts, United States). For each image, the treatment delivery state was derived and masks for the GTV and Boundary were generated by decomposing the image according to the three channels red, blue and green. Resolution of each image was 0.68 mm \times 0.68 mm, and the PTV was reconstructed for each frame with a 2 mm margin around the Boundary.

For each patient, the amount of overlap of the GTV with the Boundary and PTV was calculated, and heat maps were generated to assess the overall position of the GTV during beam-on. System latency was studied by quantifying the different states during the delivery. Its impact on the accuracy of the delivery was determined by subtracting the Gating OFF/Beam ON frames from the total amount of Beam ON frames.

3. Results

All 10 patients successfully completed the OSS procedure in one day. Nine patients were treated in inspiration, and one patient in expiration breath-hold. There was no significant difference between the average GTV delineated on the MRI and CT (4.3 cm³ vs 4.3 cm³, $p = 0.91$). Fig. 2 shows the time taken by each patient for each of the steps. Median duration of the individual steps was 0.3 h (consultation), 1.1 h (simulation), 2.8 h (planning, including plan review and approval) and 1.2 h (delivery), with an overall duration for the whole procedure of 6.6 h, which included waiting time between the different steps. Times spent in treatment planning were gradually reduced by the use of semi-automatic OAR contour delineation and pre-treatment planning on a previous diagnostic CT of the patient. This led to an overall reduction of the time needed to complete the OSS procedure, as it can be observed for patients 8, 9 and 10 (see also Supplementary Fig. 2).

Fig. 3 shows heatmaps of the GTV position during beam-on for all 10 patients (gating boundary displayed in light yellow and PTV in green). Irrespective of the size, shape, tumor motion pattern and location of the lesion, each individual heatmap clearly shows the GTV was overall well

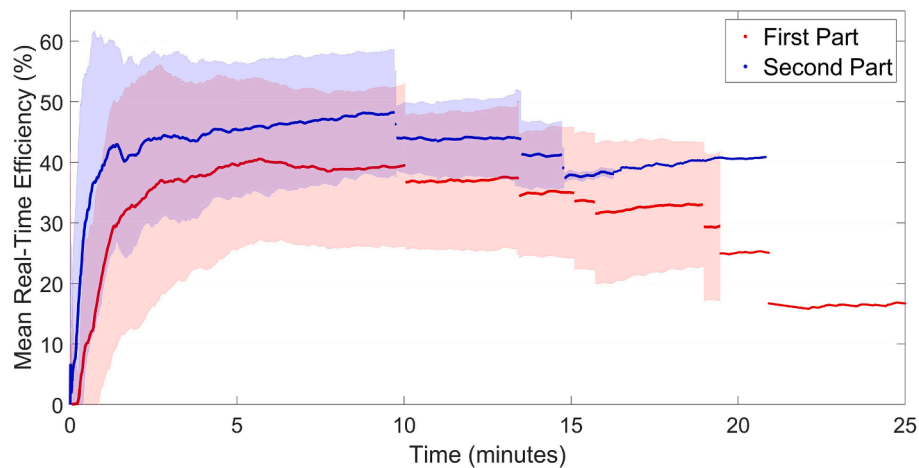


Fig. 4. Average real-time duty-cycle curves for the two parts of treatment delivery. Both curves are composed of 10 “segments”, each one displaying the average efficiency at that point in time for the remaining patients (first segment includes 10 patients, the second 9 patients, etc.). Shaded areas represent the standard deviation for each of the segments (see also Supplementary Fig. 3, for the individual curves for each patient).

centered during beam-on, thereby indicating that all patients were able to reproduce their original breath-holds. Although the GTV was located inside the gating boundary during beam-on for the majority of the time, limited portions of the GTV were also located between the gating boundary and the PTV for a relative small number of frames.

Table 2 shows a quantitative analysis of the treatment delivery accuracy and performance for the 10 patients. Whereas the 5th percentile for the overlap of the GTV with the gating boundary during beam-on ranged from 78.0 to 93.1 % for all patients, use of a 5 mm PTV margin improved this range to 94.4–100 %, leading to a better coverage of the GTV during beam-on. The frames affected by the system latency before triggering a beam-off (frames with Gating OFF/Beam ON), led to an average reduction of the overlap of the GTV with the PTV, ranging from 0.0 to 0.8 % for all patients. The overall duty-cycle of treatment delivery ranged from 26.1 to 64.7 % for all patients. Finally, the amount of frames affected by latency varied between patients, with the number of frames affected by triggering a beam-on (Gating On, but still Beam OFF) exceeding the frames affected by triggering a beam-off (Gating OFF, but still Beam ON).

An improvement in the duty-cycle of the treatment delivery was generally observed during the second part of SF treatments. Fig. 4 shows the average curves for the real-time duty-cycle of the treatment delivery for both parts. After an initial rise in the duty-cycle, a steady state is achieved which is on average higher during the second part leading to a faster delivery. The individual curves for each of the patients are supplied in the Supplementary Fig. 3.

All ten patients expressed their overall satisfaction with the PREMs collected after completion of the treatment (see also, Supplementary Fig. 4). Patients who had to wait longer between different steps indicated less satisfaction than those in whom the procedure could be completed within a half day.

4. Discussion

Single fraction SABR is an effective treatment option for small lung tumors [4–6]. We extended this work by implementing a single visit MR-guided OSS SABR service. The findings of the present study, where all patients completed the procedure in a single day, revealed an overall high patient satisfaction. Furthermore, refinements in our workflow reduced patient time in hospital to just a half day. These reductions in time were achieved in the treatment planning process by use of semi-automatic contouring of OARs, and performing pre-planning on available diagnostic-CT scans.

Our use of a dedicated simulation procedure during which tumor

motion characteristics were assessed to (i) identify a suitable breath-holding phase for the patient, and (ii) performing GTV contour “tracking” for auto-beam gating, provided the patients with an opportunity to gain confidence in the video-assisted delivery procedure. Duty-cycle efficiencies varied considerably among all patients, with averages for the whole treatment ranging from 26.1 % to 64.7 %. These numbers are somewhat lower than those reported previously for larger lung tumors [13]. This can be attributed to smaller GTVs and the inclusion of the CV threshold in this study. Treatment delivery was split in two parts to allow the patient to take some rest due to repeated breath-holding, being especially relevant in our patient population with a median age of 71 years (see also Table 1). This split also limited the need for patients to lie completely still during prolonged delivery. The second phase of SABR delivery was faster for the majority of our patients, with higher duty-cycle efficiencies and evidence for a learning curve for the patients.

MR-guided SABR allowed continuous intra-fraction monitoring of the anatomy of the patient during treatment delivery. MR-cines collected at 0.35 T with the MRidian system provided good image quality even for small tumors of 1–2 cm³. The ability to perform gated delivery with beam delivery control based on the visualization of soft tissue ensured accurate treatments. Our implementation relied on the combination of two possible thresholds for triggering a beam-off: 1) the area of the GTV falling outside the gating boundary; 2) a CV metric which provides information about the reliability of the online DIR and auto-contouring of the GTV for each frame. Failure of one of the two conditions led to triggering beam-off events and fulfilment of both again to beam-on events. A substantial, but variable, number of frames were affected by system latency, ranging from 5.3–18.1 % (Gating ON/Beam OFF) and 2.2–8.2 % (Gating OFF/Beam ON). Both reduced the overall duty-cycle efficiency and are dependent on patient compliance with breath-holding, and the thresholds chosen for triggering the beam-off/on events.

To minimize the impact of system-latency on the accuracy of treatment delivery without compromising treatment margins, we used a gating boundary structure of 3 mm and a PTV margin of 5 mm around the GTV. This approach led to an overall improvement of the GTV area covered during beam-on, with on average at least 94.4 % (5th percentile) of the GTV always present inside of the PTV during beam-on. For all patients it was possible to use the GTV contour as reliable “tracking” structure, although it might have been possible as well to use other surrogate structures.

One shortcoming of our study is the short median patient follow-up. However, previous studies reporting on SF lung delivery have shown equivalent clinical outcomes to fractionated lung SABR [4,6,17]. In

addition, Finazzi et al. reported recently no CTCAE grade 3–5 toxicities and no local recurrences for SF lung MR-guided SABR [14].

Our approach can however only be applied to relative small tumors (<5cm diameter) and not in the proximity of sensitive structures in the thoracic region. However, the same-day simulation and treatment planning/delivery may be an attractive option for those patients who need to travel long distances for treatment and fulfilling the eligibility criteria. Our approach is now being extended to other disease sites, including the abdomen, where MRgRT can provide excellent image quality [13,18]. However, care should be taken when OARs are in close proximity to the target as online plan adaptation may play a more important role to ensure a safe delivery.

Declaration of Competing Interest

The authors declare that they have no known competing financial interests or personal relationships that could have appeared to influence the work reported in this paper.

Appendix A. Supplementary data

Supplementary data to this article can be found online at <https://doi.org/10.1016/j.phro.2022.09.010>.

References

- [1] Postmus PE, Kerr KM, Oudkerk M, Senan S, Waller DA, Vansteenkiste J, et al. Early and locally advanced non-small-cell lung cancer (NSCLC): ESMO Clinical Practice Guidelines for diagnosis, treatment and follow-up. *Ann Oncol* 2017;28. <https://doi.org/10.1093/annonc/mdx222>. iv1–21.
- [2] Roach MC, Bradley JD, Robinson CG. Optimizing radiation dose and fractionation for the definitive treatment of locally advanced non-small cell lung cancer. *J Thorac Dis* 2018;10:S2465–673. <https://doi.org/10.21037/jtd.2018.01.153>.
- [3] Guckenberger M, Andratschke N, Dieckmann K, Hoogeman MS, Hoyer M, Hurkmans C, et al. ESTRO ACROP consensus guideline on implementation and practice of stereotactic body radiotherapy for peripherally located early stage non-small cell lung cancer. *Radiother Oncol* 2017;124:11–7. <https://doi.org/10.1016/j.radonc.2017.05.012>.
- [4] Singh AK, Gomez-Suescun JA, Stephans KL, Bogart JA, Hermann GM, Tian L, et al. One versus three fractions of stereotactic body radiation therapy for peripheral stage i to ii non-small cell lung cancer: A randomized, multi-institution, phase 2 trial. *Int J Radiat Oncol Biol Phys* 2019;105:752–9. <https://doi.org/10.1016/j.ijrobp.2019.08.019>.
- [5] Videtic GM, Paulus R, Singh AK, Chang JY, Parker W, Olivier KR, et al. Long-term follow-up on NRG oncology RTOG 0915 (NCCTG N0927): a randomized phase 2 study comparing 2 stereotactic body radiation therapy schedules for medically inoperable patients with stage i peripheral non-small cell lung cancer. *Int J Radiat Oncol Biol Phys* 2019;103:1077–84. <https://doi.org/10.1016/j.ijrobp.2018.11.051>.
- [6] Siva S, Bressel M, Mai T, Le H, Vinod S, de Silva H, et al. Single-Fraction vs multifraction stereotactic ablative body radiotherapy for pulmonary oligometastases (SAFRON II). *JAMA Oncol* 2021;7:1476–85.
- [7] Videtic GMM, Stephans KL, Woody NM, Reddy CA, Zhuang T, Magnelli A, et al. 30 Gy or 34 Gy? comparing 2 single-fraction SBRT dose schedules for stage i medically inoperable non-small cell lung cancer. *Int J Radiat Oncol Biol Phys* 2014;90:203–8. <https://doi.org/10.1016/j.ijrobp.2014.05.017>.
- [8] Finazzi T, Haasbeek CJA, Spoelstra FOB, Palacios MA, Admiraal MA, Bruynzeel AME, et al. Clinical outcomes of stereotactic MR-guided adaptive radiation therapy for high-risk lung tumors. *Int J Radiat Oncol Biol Phys* 2020;107:270–8. <https://doi.org/10.1016/j.ijrobp.2020.02.025>.
- [9] Finazzi T, Palacios MA, Spoelstra FOB, Haasbeek CJA, Bruynzeel AME, Slotman BJ, et al. Role of on-table plan adaptation in mr-guided ablative radiation therapy for central lung tumors. *Int J Radiat Oncol Biol Phys* 2019;104:933–41. <https://doi.org/10.1016/j.ijrobp.2019.03.035>.
- [10] Bayasgalan U, Moon SH, Jeong JH, Kim TH, Cho KH, Suh YG. Treatment outcomes of passive scattering proton beam therapy for stage I non-small cell lung cancer. *Radiat Oncol* 2021;16:1–9. <https://doi.org/10.1186/s13014-021-01855-w>.
- [11] Gomez DR, Li H, Chang JY. Proton therapy for early-stage non-small cell lung cancer (NSCLC). *Transl Lung Cancer Res* 2018;7:199–204. <https://doi.org/10.21037/tlcr.2018.04.12>.
- [12] Henke LE, Olsen JR, Contreras JA, Curcuro A, DeWees TA, Green OL, et al. Stereotactic MR-guided online adaptive radiation therapy (SMART) for ultracentral thorax malignancies: results of a phase 1 trial. *Adv Radiat Oncol* 2019;4:201–9. <https://doi.org/10.1016/j.adro.2018.10.003>.
- [13] van Sörnsen de Koste JR, Palacios MA, Bruynzeel AME, Slotman BJ, Senan S, Lagerwaard FJ. MR-guided gated stereotactic radiation therapy delivery for lung, adrenal, and pancreatic tumors: a geometric analysis. *Int J Radiat Oncol Biol Phys* 2018;102:858–66. <https://doi.org/10.1016/j.ijrobp.2018.05.048>.
- [14] Finazzi T, van Sörnsen de Koste MA, Palacios MA, Spoelstra FOB, Slotman BJ, Haasbeek CJA, et al. Delivery of magnetic resonance-guided single-fraction stereotactic lung radiotherapy. *Phys Imaging. Radiat Oncol* 2020;14:17–23. <https://doi.org/10.1016/j.phro.2020.05.002>.
- [15] Brunenberg EJJ, Kusters JMAM, Van Kollenburg PGM, Braam PM. SP-0469: The development of a one-stop-shop palliative radiotherapy treatment using MR and CBCT. *Radiother Oncol* 2014;111:S183–4. [https://doi.org/10.1016/s0167-8140\(15\)30574-0](https://doi.org/10.1016/s0167-8140(15)30574-0).
- [16] Benson R, Clough A, Nelder C, Pitt E, Portner R, Vassiliou M, et al. Evaluation of the palliative radiotherapy pathway in a single institute: Can an MR Linac improve efficiency? *J Med Imaging Radiat Sci* 2021;53:44–50. <https://doi.org/10.1016/j.jmir.2021.11.010>.
- [17] Videtic GMM, Reddy CA, Woody NM, Stephans KL. Ten-year experience in implementing single-fraction lung SBRT for medically inoperable early-stage lung cancer. *Int J Radiat Oncol Biol Phys* 2021;111:436–42. <https://doi.org/10.1016/j.ijrobp.2021.05.116>.
- [18] Mazur TR, Fischer-Valuck BW, Wang Y, Yang D, Mutic S, Li HH. SIFT-based dense pixel tracking on 0.35 T cine-MR images acquired during image-guided radiation therapy with application to gating optimization. *Med Phys* 2016;43:279. <https://doi.org/10.1118/1.4938096>.